
One Loss to Rule Them All: Marked Time-to-Event for Structured EHR Foundation Models

Zilin Jing¹ Vincent Jeanselme² Yuta Kobayashi² Simon A. Lee³ Chao Pang^{2,4} Aparajita Kashyap²
Yanwei Li² Xinzhuo Jiang² Shalmali Joshi²

Abstract

Clinical events captured in Electronic Health Records (EHR) are irregularly sampled and may consist of a mixture of discrete events and numerical measurements, such as laboratory values or treatment dosages. The sequential nature of EHR, analogous to natural language, has motivated the use of next-token prediction to train prior EHR Foundation Models (FMs) over events. However, this training fails to capture the full structure of EHR. We propose *ORA*, a marked time-to-event pretraining objective that jointly models event timing and associated measurements. Across multiple datasets, downstream tasks, and model architectures, this objective consistently yields more generalizable representations than next-token prediction and pretraining losses that ignore continuous measurements. Importantly, the proposed objective yields improvements beyond traditional classification evaluation, including better regression and time-to-event prediction. Beyond introducing a new family of FMs, our results suggest a broader takeaway: pretraining objectives that account for EHR structure are critical for expanding downstream capabilities and generalizability.

1. Introduction

Large-scale FMs have shifted the paradigm of machine learning in health by extracting representations that transfer across tasks, cohorts, and institutions (Guo et al., 2023; 2024; Lee et al., 2024; Burkhart et al., 2025). Inspired by the success of large language models (LLMs), recent work has framed Electronic Health Records (EHR) as sequences of discrete events typically pretrained using next-token predi-

tion analogous to those used in natural language processing. These approaches have demonstrated state-of-the-art performance on a range of downstream classification tasks (Li et al., 2020; Pang et al., 2024; 2021; Odgaard et al., 2024).

Despite these advances, EHR data fundamentally differ from natural language in ways that challenge this analogy. Clinical records are not sequences of tokens. Instead, they consist of heterogeneous medical events occurring at irregular time intervals, often accompanied by numerical measurements. To address these challenges, most FMs design customized tokenizations, including artificial time tokens and time embeddings (Pang et al., 2024) for irregularity, discretized intervals (Wornow et al., 2024a), and digit space embedding (Hur et al., 2023) for numerical value. However, these modifications focus on how data should be represented as input and often overlook how these aspects should influence the design of EHR pretraining losses.

Next-token prediction is a coarse surrogate for the underlying clinical process. Recent literature (Steinberg et al., 2024; Gadd et al., 2025; Burger et al., 2025) proposed time-to-event pretraining loss as an alternative, with Gadd et al. (2025); Burger et al. (2025) additionally introducing pretraining objectives that capture numerical values. However, these works often introduce disparate architectural choices, preprocessing and tokenization strategies while also introducing new pretraining losses. As a result, the impact of the pretraining loss design has been obscured and challenging to isolate. Our work aims to answer: *Does a loss function accounting for EHR irregularity and numerical values yield more generalizable representations than the existing approaches?*

To answer this question, we propose *ORA*, a marked time-to-event pretraining objective that jointly models the distribution of event timing and associated measurements for each medical code, naturally handling irregular intervals, censoring, and associated numerical values, if present. We further expand downstream evaluation to characterize time-to-event and regression performance on multiple clinically meaningful tasks (Pang et al., 2025), beyond prior work that focuses on classification tasks. Across two large EHR datasets, representing large tertiary and quaternary healthcare insti-

¹Department of Computer Science, Columbia University, New York, USA ²Department of Biomedical Informatics, Columbia University, New York, USA ³Department of Computational Medicine, UCLA, Los Angeles, USA ⁴Formation Bio. Correspondence to: Zilin Jing <zj2398@columbia.edu>.

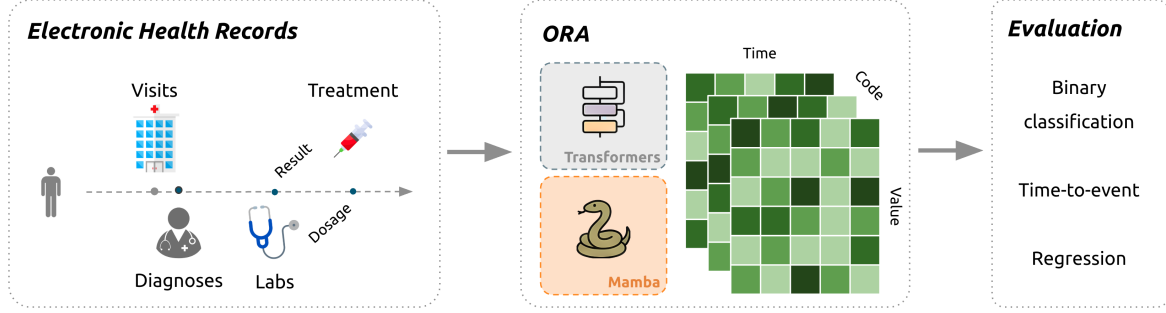


Figure 1. Our work introduces ORA, a marked time-to-event pretraining loss that accounts for the value and irregular timing of EHR, demonstrating the importance of the loss design for improved downstream capabilities and generalizability.

tutions, we extensively evaluate the pretraining objective across 14 tasks. Our experimentation with Transformer and Mamba architectures demonstrates improved performance of 10.7% and 11.4%, respectively, on average across 7 classification, 3 regression, and 4 time-to-event tasks. Critically, we demonstrate that this objective is effective across multiple architectures, including Transformers and Mamba, and that these FMs yield superior performance across multiple sites. Together, these results provide a critical insight into the design of future FMs: pre-training objectives must align with the full structure of EHR to ensure more expressive and generalizable models. Our contributions can be summarized as follows:

- **Novel loss.** Building on the parallel between EHR and marked point processes (Section 3), we introduce ORA, a composite code-specific likelihood to capture EHR complexity.
- **Generalizability.** We demonstrate improved generalizability of ORA on top of both Mamba and Transformer base models (Section 4) across tasks and datasets.
- **Comprehensive Downstream Task Evaluation.** Our experiments include 7 binary classification, 4 time-to-event prediction, and 3 regression tasks across two datasets. Our results demonstrate that ORA improves performance in diverse clinically-meaningful tasks.

2. Related Work

This section reviews FMs for structured EHR data, with an emphasis on how the literature adapts natural language strategies to model clinical data. We then examine the training objectives inherited from this field and discuss alternatives.

Foundation models for structured EHR. Echoing the success of language models, FMs have emerged as an effective paradigm in structured EHR modeling (Wornow et al., 2023; Steinberg et al., 2021; Odgaard et al., 2024; Pang et al., 2025; Cui et al., 2025; Steinberg et al., 2024; Wornow et al.,

2024a; Gadd et al., 2025; Burger et al., 2025; Shmatko et al., 2025; Wornow et al., 2024b). Instead of task-specific models, FMs are pretrained on large amounts of structured EHR to extract representations with the goal of linear-probe predictive capabilities (Pang et al., 2025). We refer the reader to Ren et al. (2025) for an extensive survey of structure and unstructured EHR FMs, and focus this review on how the key differences between EHR from natural language.

EHR data is characteristically marked by irregular time points and may include numerical values, such as the time of measurement and the corresponding result. Ignoring these dimensions discards important proxies of patients’ health (Jeanselme, 2024), potentially reducing the representativeness of FMs.

EHR representation. Two key alternatives have been proposed to represent these different dimensions in a format amenable to training FMs: serialization and tokenization. First, the availability of text-based general-purpose LLMs has spurred work in training representations using text-serialized EHR data (Su et al., 2025; Hegselmann et al., 2025; 2023; Lee et al., 2024; 2025; Cui et al., 2025). While our findings may provide insights for training such models, we focus on explicit tokenization of structured EHR elements, which represents the sequence of diagnosis codes, procedures, prescriptions, labs, and visit information as tokens using clinically relevant vocabularies (Hripcsak et al., 2019), as opposed to natural language vocabularies. For instance, BEHRT (Li et al., 2020), Med-BERT (Rasmy et al., 2021), CEHR-BERT (Pang et al., 2021) and variants (An et al., 2025; Shmatko et al., 2025) leverage such token sequences to train BERT architectures (Devlin et al., 2019). More recently, decoder-based approaches reframe EHR modeling using next-token prediction (Pang et al., 2024). Beyond standard transformer architectures, state-space models like Mamba (Gu & Dao, 2023) have also been used to model EHR sequences, and demonstrate strong generalizability across different downstream tasks (Fallahpour et al., 2024; Wornow et al., 2024a).

However, the challenge associated with time and value re-

mains in this tokenization. To handle irregular medical events, CEHR-BERT (Pang et al., 2021) introduces artificial time tokens as input. MOTOR (Steinberg et al., 2024) uses rotary position embeddings to integrate time in the attention mechanism. For numerical value encoding, Wornow et al. (2024a) discretizes numerical code into tokens. Alternatively, Hill et al. (2023) assigns measurement to a unique embedding.

An inherited pretraining loss from natural language. The parallel between medical event streams and words in a sentence has not only influenced the way to represent EHR but also to train such models (McDermott et al., 2023). Particularly, FMs’ training often relies on maximizing the likelihood of the next token. Even in the more general context of time series, FMs often minimize this loss (Ansari et al., 2024) or the mean square error of the next value (Jin et al., 2023; Goswami et al., 2024; Chang et al., 2025a; Das et al., 2024), implicitly assuming temporal regularity in observation sequences. Such losses do not account for the temporal irregularities and associated values characteristic of EHR, a problem that has largely been overlooked in the development of FMs.

Marked point process. In statistics, irregularly sampled time series are typically modeled using temporal point processes. When events are associated with values, a marked point process captures the underlying stochastic process (Snyder & Miller, 2012; Daley & Vere-Jones, 2003). Prior work has explored improving predictive models by modeling EHR event types jointly with their occurrence times, often through point-process formulations (Du et al., 2016; Enguehard et al., 2020; Bhave & Perotte, 2021; Islam et al., 2017; Schulam & Saria, 2017; Alaa et al., 2017). More recent FMs extend this idea by introducing time-to-event pretraining objectives that require predicting not only which event occurs next, but also when it occurs (Karami et al., 2024; Steinberg et al., 2024; Chang et al., 2025b; Shmatko et al., 2025). Most closely related to our work, a couple of FMs model event-associated values (Gadd et al., 2025; Burger et al., 2025). However, the variability in tokenization strategies and architectural differences has made it challenging to isolate the impact of the choice of pretraining loss on downstream performance. Prior benchmarking evaluates performance gains in linear-probe classification tasks, demonstrating inconsistent gains and limited transportability across clinically meaningful predictions and models (Pang et al., 2025; Wornow et al., 2024b). In contrast, our work isolates the role of the pretraining objective, while expanding downstream evaluation to linear-probe regression and time-to-event prediction.

3. EHR as marked point process

EHR data quintessentially consists of irregularly sampled temporal events, which may or may not be associated with numerical values, either discrete or continuous. To fully capture its characteristics, we propose to jointly model the value and observation time for each code given patient history.

We consider each patient $i \in [1, 2, \dots, N]$ ’s EHR data to consist of a tuple $\mathcal{H}_i := \{(t, m, v)_{i,j}, j \in [1, 2, \dots, N_i]\}$ where $t \in \mathbb{R}^+$, is the timestamp of the event, $m \in \mathcal{M}$ the clinical code associated with the event, such as ICD-10 diagnosis or procedure codes, and $v \in \mathbb{R}$ the optional numerical value associated with the event. N_i denotes the number of events observed for patient i . For a patient i , events up to j (ordered by time) are denoted by $\mathcal{H}_{i,<j}$. That is, $\mathcal{H}_{i,<j} := \{(t, m, v)_{i,l}, l \in [1, 2, \dots, j-1]\}$. Finally, we denote by $f_{i,j}^m$, the first occurrence of code m after the time associated with event j , and the set of the first events of all codes as $\mathcal{F}_{i,j} = \{\forall m, f_{i,j}^m\}$. Specifically, we define:

$$f_{i,j}^m = (\Delta t_j^m, v, \delta, m)$$

where, if an event of type m occurs after t_j , Δt_j^m corresponds to the interval between the current time t_j and the time to the next event m , and $\delta = 1$ as an event indicator. If no such event occurs in the future, we denote Δt_j^m as the interval up to the last observation, and set the event indicator to $\delta = 0$. In this context, δ denotes whether an event m is observed within the recorded EHR for patient i after the observation j or censored. Accounting for such unobserved events is critical, as ignoring them leads to biased likelihood estimates (Chen et al., 2024).

Joint likelihood. We propose a pretraining loss to learn generalizable representations of patient EHR. An intuitive approach is to maximize the joint likelihood of the full marked point process, corresponding to the joint between the time to the next event, the associated code, and value. Under standard IID assumptions on patient samples, the joint likelihood can be decomposed as:

$$\mathcal{L}(\theta) = \prod_{i=1}^N p_\theta(\mathcal{H}_i) = \prod_{i=1}^N \prod_{j \in [1..N_i]} p_\theta((t, m, v)_{i,j} | \mathcal{H}_{i,<j})$$

However, maximizing this joint likelihood poses some challenges:

- **Mismatch between token (mark)-level autoregressive prediction and downstream tasks.** Clinically meaningful downstream tasks often involve representations composed of multiple codes rather than a single one. For example, disease phenotyping is often characterized by multiple (potentially temporally ordered) codes, combined with conditions on their values (e.g., abnormal lab results). Simply optimizing the next-event loss may miss this multiplicity, reducing

meaningful and long-term representativeness and failing to capture the patient’s health evolution.

- **Sparse supervision.** In autoregressive next-event modeling, only the next observed event impacts the likelihood, even though many future clinical events could occur. This yields a sparse learning signal with rare events having a limited impact on the overall likelihood.
- **Mutual exclusivity.** The joint likelihood assumes that if one event is observed, it precludes all others. In practice, multiple events are often observed simultaneously, which calls into question this assumption.

ORA. To address these challenges, we instead propose to optimize the composite code-specific likelihood. At each observation j , we jointly model the first occurrence time and the value of every code, assuming conditional independence of the codes given the contextual history $\mathcal{H}_{i,<j}$ of the patient:

$$\tilde{\mathcal{L}}_{\text{ORA}}(\theta) = \prod_i \prod_j \prod_{(\Delta t, m, v, \delta) \in \mathcal{F}_{i,j}} p_{\theta_m}(\Delta t, v, \delta \mid \mathcal{H}_{i,<j}) \quad (1)$$

Formally, this corresponds to a code-specific marked point process. Beyond accounting for uncertainty in the health-care process, this formulation empirically allows the use of all potential next events at a given time point, thereby overcoming the sparsity of observations and improving data efficiency. In contrast to [Steinberg et al. \(2024\)](#), which models the time-to-event assuming conditional independence, our work models the time-to-event and associated (optional) value jointly. The proposed approach differs from [Burger et al. \(2025\)](#), which describes a conditional temporal process based on values, i.e. $p_{\theta_m}(\Delta t, \delta \mid \mathcal{H}_{i,<j}, v)$. While the latter allows to estimate when an event of a certain value may occur, it does not estimate the full joint. Closest to our work, [Gadd et al. \(2025\)](#) assumes conditional independence between the value and time under a parametric assumption.

4. Implementing ORA

The previous section introduces ORA to train FMs. This section describes how to modify different architectures to maximize this loss.

4.1. Discretized ORA

The central challenge in computing the proposed loss (Eq. (1)) is the estimation of $p_{\theta_m}(\Delta t, v, \delta \mid \mathcal{H}_{i,<j})$, or equivalently, under the conditional independence and the common uninformative censoring assumptions:

$$\begin{aligned} \log p_{\theta_m}(\Delta t, v, \delta \mid \mathcal{H}_{i,<j}) \\ = \delta \log \lambda_{\theta_m}(t, v \mid \mathcal{H}_{i,<j}) - \int_0^t \int_{v'} \lambda_{\theta_m}(u, v' \mid \mathcal{H}_{i,<j}) dv' dt' \end{aligned}$$

where $\lambda_{\theta_m}(\cdot)$ is the instantaneous risk, or intensity function, of observing an event associated with code m .

Estimating the likelihood, therefore, requires modeling the instantaneous risk and its integral for each code m . Approaches in survival analysis and temporal point analysis often constrain the intensity function to have a closed-form integral through parametric assumptions ([Du et al., 2016](#); [Mei & Eisner, 2017](#)) or through constrained neural networks ([Omi et al., 2019](#); [Jeanselme et al., 2023](#)). In this work, we adopt a discretization of the joint, extending survival approaches such as DeepHit ([Lee et al., 2018](#)) to marked point processes. While approximating the likelihood, this approach has shown to be computationally efficient and to achieve state-of-the-art performance in survival analysis ([Lee et al., 2018](#)). Concretely, we add a final network layer to model the discretized joint distribution over time-value tuples. For each code m and input x , the neural network outputs a matrix $P^m(x) \in [0, 1]^{T \times V}$, a discretized approximation of the intensity function, where T and V denote the number of discretized bins for time and value, respectively. Each entry $P^m[k, l]$ represents the probability of observing an event in the k^{th} time-quantile and l^{th} value-quantile. Let $q_m(t, v)$ return the time-value quantiles associated with code m to which (t, v) belongs. When v is omitted, $q_m(t, \cdot)$ denotes the time-quantile. Under this discretization, the log-likelihood can be expressed as:

$$\begin{aligned} \log \tilde{\mathcal{L}}_{\text{ORA}}(\theta) := \sum_{i=1}^N \sum_{j \in [1 \dots N_i]} \sum_{(t, m, v, \delta) \in \mathcal{F}_{i,j}} \\ \delta \log P_{\theta}^m[q_m(t, v)](\mathcal{H}_{i,<j}) \\ + (1 - \delta) \log \left(1 - \sum_{k=1}^{q_m(t, \cdot)} \sum_l P_{\theta}^m[k, l](\mathcal{H}_{i,<j}) \right) \end{aligned}$$

For observed events, this objective maximizes the probability mass assigned to the quantile containing the time and value of the next event. For censored events, it enforces a low probability of observing any event before the end of the observation window, marginalizing over all possible values.

4.2. Model Design

To maximize the previous likelihood, one must extract a representation of the medical history $\mathcal{H}_{i,<j}$ and compute the matrix $P^m(x)$. Importantly, the proposed pre-training loss is architecture agnostic. We propose evaluating its efficacy on common FMs architectures: an attention-based architecture (Transformer ([Vaswani et al., 2017](#))) and a state-space model (Mamba ([Gu & Dao, 2024](#))) to demonstrate its utility for modeling EHR data.

EHR tokenization. To isolate the effects of the loss on performance, we fix the tokenizer to the one developed by [Steinberg et al. \(2024\)](#) and adopt a similar entropy-based

filter to construct the vocabulary with the most informative events. Specifically, we quantify the informativeness of each code using its empirical entropy, and retain codes with the highest entropy to reduce noise in the learning process. More details can be found in Appendix A.3.1.

Backbone. Following Steinberg et al. (2024), we adopt a decoder-only Transformer backbone that avoids look-ahead from future medical events through a causal attention mechanism. Unlike the standard Transformer, it uses rotary position embeddings with age for improved temporality processing. It also adopts local attention and sample packing for efficient pretraining.

As an alternative, we train Mamba, a state-space model introduced in Gu & Dao (2024), using the proposed pretraining loss. Mamba replaces attention-based modules in the Transformer with a selective state-space block, whose compute time scales linearly with sequence length. Prior work has shown its advantage over the Transformer in capturing long, irregular EHR sequences with temporal dependencies (Wornow et al., 2024a; Fallahpour et al., 2024).

Efficient projection head. The last layer of our architectures includes a head to project the output embedding $E \in \mathbb{R}^D$, with D is the model’s hidden dimension, to the probability matrix $\forall m \in \mathcal{M}, P^m(x) \in (0, 1)^{T \times V}$. A direct projection from \mathbb{R}^D to the discretized joint of shape $T \times V \times |\mathcal{M}|$ would require an impractical number of parameters to estimate. Instead, following (Steinberg et al., 2024), we use a factorized two-stage computation. First, a one-layer fully connected neural network projects the embedding E to time-specific features $H_j \in \mathbb{R}^{T \times D_2}$. Then we use a second projection followed by a final Softmax for all codes with numerical values, projecting H_j into the final matrix $P^m \in [0, 1]^{T \times V}$. Similarly, for nonnumerical codes, a single-layer project into $P^m \in [0, 1]^{T \times 1}$.

In our experiments, we use $D = 768$, $D_2 = 512$, $T = 8$, $V = 10$, and $|\mathcal{M}| \approx 7000$. This factorization reduces the number of parameters by 20% compared to a fully connected network that projects the embedding onto the discretized joint. Full architectural details and exact tensor shapes are provided in Appendix A.3.3. All models are trained with a fixed 120M-parameter budget; model configurations are listed in Appendix A.3.2.

5. Experiments

Our experiments characterize the impact of the choice of pretraining loss on the representativeness of extracted embeddings. We compare three types of losses across two architectures and conduct linear probing to evaluate performance on 14 tasks across two EHR datasets.

5.1. Datasets

We rely on one public EHR dataset: MIMIC-IV (Johnson et al., 2023) and a private EHR dataset from Columbia University Irving Medical Center (CUMC). MIMIC-IV contains 364,000 patients who were admitted to Beth Israel Deaconess Medical Center between 2008 and 2022, with tabular time-series measurements of diagnoses, medications, lab tests, etc. The CUMC dataset contains 6.7 million patients with both inpatient and outpatient visits, primary care, and emergency services between 1986 and 2023, consisting of diagnoses, procedures, medications, and visit information (see Appendix A.1 for patient split used for pretraining). Additional details about tokenization, architecture design, and hyperparameter tuning are in Appendix A.3.

5.2. Downstream Tasks

To ensure clinical utility, we design a set of clinically meaningful downstream tasks that encompass binary classification, time-to-event prediction, and regression of lab tests.

Binary Classification. We consider 7 binary classification tasks from Pang et al. (2025), representing prognosis of:

- Three patient outcomes: In-hospital mortality (Mortality), a length of stay longer than 7 days (LOS), and 30-day readmission (Readmission).
- Two chronic conditions: Celiac and Metabolically Associated Steatotic Liver Disease (MASLD).
- Two acute conditions: Acute Myocardial Infarction (AMI) and Ischemic Stroke (Stroke).

The detailed definition of phenotype diseases can be found in Appendix A.2.2. Predicting chronic and acute conditions is particularly challenging because of the considered ‘at-risk’ cohort, which increases task difficulty while improving downstream clinical utility. We treat chronic conditions as incident onset events and therefore evaluate only the first occurrence, consistent with clinical interest in early identification. In contrast, acute conditions may recur, so we include all occurrences and formulate a recursive prediction task to capture repeated risk over time.

Time-to-event. Clinical decision-making often depends not only on whether an event will occur, but also on when it is expected to occur. To evaluate this capability, we consider time-to-event prediction for four conditions (Celiac, MASLD, AMI, and Stroke). For each condition, the prediction time is defined at the discharge of an inpatient visit, and the task is to predict the time until the patient receives the first diagnosis of the corresponding condition.

Regression. Comprehensive characterization of patient health requires predicting future physiological measurements. Prior works have largely overlooked regression and

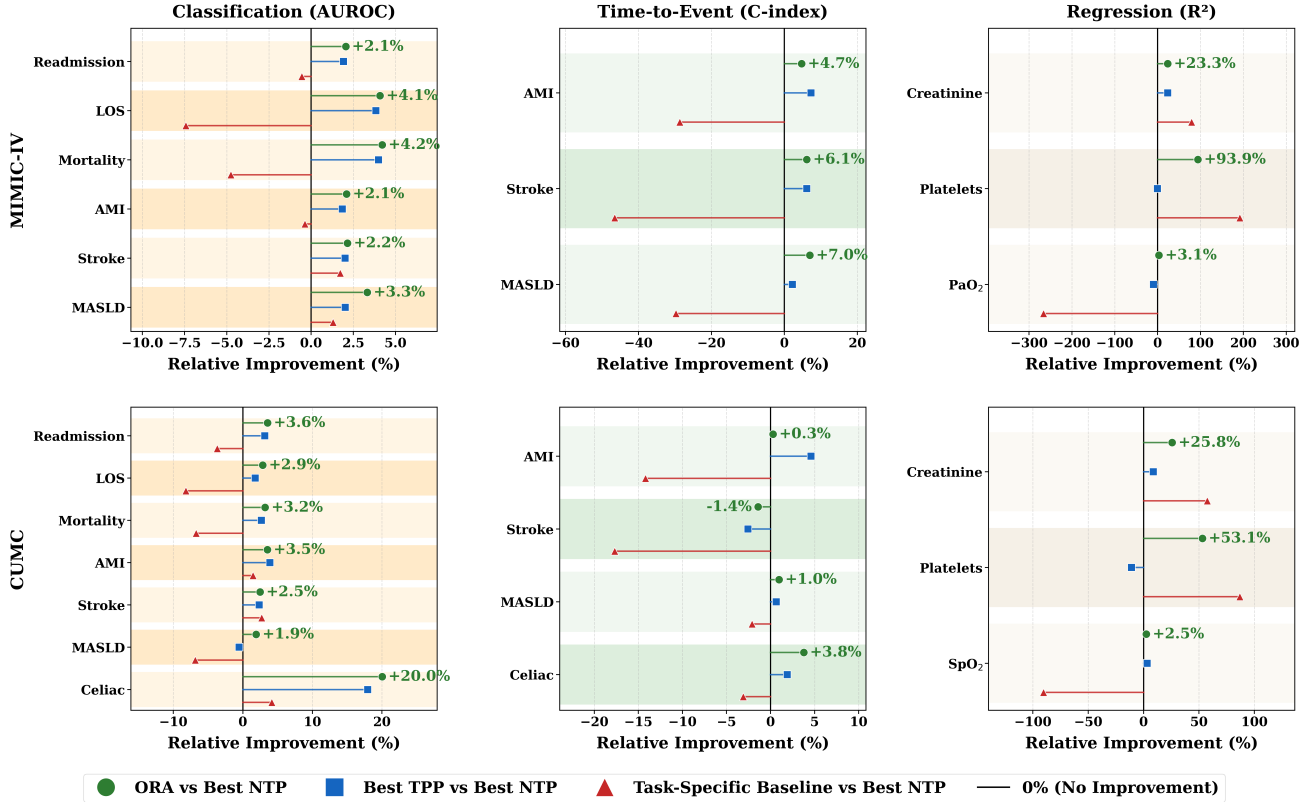


Figure 2. Relative improvement (%) over the strongest Next-Token Prediction (NTP) baseline on each task for the **Transformer** architecture. For each dataset (MIMIC-IV and CUMC), we compare ORA (green circles), the best Temporal Point Process (TPP) pretraining model (blue squares), and task-specific supervised baselines (red triangles) across classification, time-to-event, and regression tasks.

time-to-event as downstream tasks. We assess FM performance on regression tasks involving three laboratory measurements used in the computation of the SOFA severity score (Vincent et al., 1996): Platelets, Creatinine, and Oxygen. Each measurement is identified by a single medical code (see Appendix A.2.3). All of them are included in the tokenizer vocabulary of each pretrained model, ensuring they are not out-of-vocabulary at evaluation time. To avoid leakage across visits, we restrict evaluation to same-visit laboratory tests that occur at least four hours after admission, and we define the prediction time to be exactly four hours before the corresponding lab event.

5.3. Baseline Models and Associated Loss

Our experiments include the following baselines and FMs:

- **Task-Specific Baselines:** For each task, we consider XG-Boost (Chen & Guestrin, 2016) for binary classification, Deephit (Lee et al., 2018) for time-to-event prediction based on FEMR features (Steinberg et al., 2024) from the EHR time series. For regression, we used the most recent value for the same lab code, measured before the prediction time.

- **Next Token Prediction (NTP):** We pretrain both Transformer and Mamba using next-token prediction (loss computed by cross-entropy), following the same tokenization and preprocessing of Steinberg et al. (2024). Using the same notations as in Section 3, NTP consists of maximizing the likelihood:

$$\mathcal{L}_{\text{NTP}}(\theta) := \prod_{i=1}^N \prod_{j \in [1..N_i]} p_{\theta}(m_{i,j} \mid \mathcal{H}_{i,<j})$$

As further baselines using NTP, we consider SOTA FMs from Context Clue (Wornow et al., 2024a): CC-Llama and CC-Mamba, which use different tokenizations but the same NTP paradigm. For each task, we report *Best NTP* as the best NTP-trained model within the same architecture (Transformer or Mamba).

- **Temporal Point Process (TPP):** As an intermediary loss, we consider a code-specific time-to-event loss that does not model the associated measurements of future observations, as proposed in Steinberg et al. (2024) (MOTOR). We use this loss on top of the Transformer and Mamba to constitute the ‘TPP’ pre-trained models. Mathematically, TPP associated

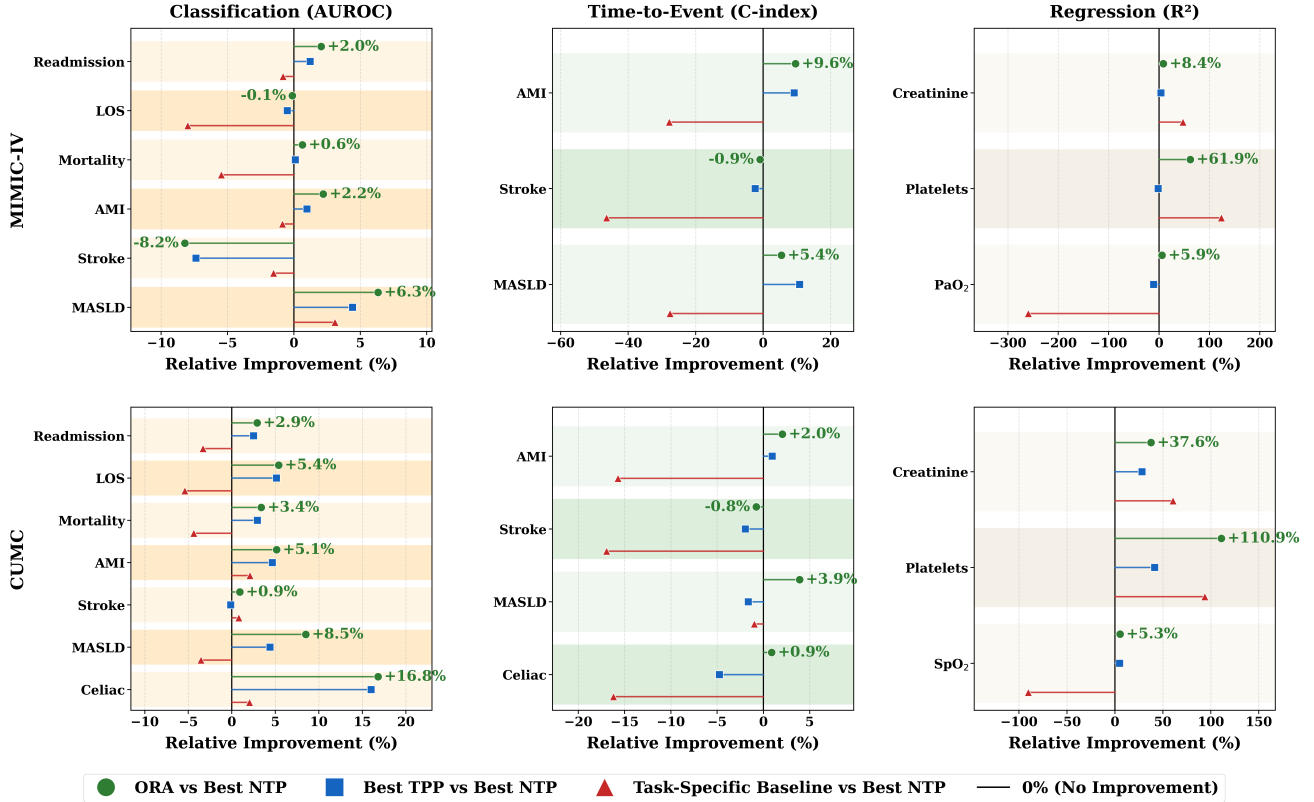


Figure 3. Relative improvement (%) over the strongest Next-Token Prediction (NTP) baseline on each task for the **Mamba** architecture. For each dataset (MIMIC-IV and CUMC), we compare ORA (green circles), the best Temporal Point Process (TPP) pretraining model (blue squares), and task-specific supervised baselines (red triangles) across classification, time-to-event, and regression tasks.

likelihood can be described as:

$$\mathcal{L}_{\text{TPP}}(\theta) := \prod_i \prod_j \prod_{(\Delta t, m, \delta) \in \mathcal{F}_{i,j}} p_{\theta_m}(\Delta t, \delta \mid \mathcal{H}_{i,<j})$$

We maximize this quantity using a discretization analogous to the one used for ORA. Additionally, we compare with the original MOTOR (Steinberg et al., 2024), which uses a piecewise exponential function to predict future events instead of the proposed discretization. For each task, we also report *Best TPP* as the best TPP-based model within the same architecture (Transformer or Mamba).

5.4. Evaluation

To quantify the discriminative performance of all models, we report the Area Under the Receiver Operating Characteristic Curve (AUROC) for classification, the time-dependent C-index (Antolini et al., 2005) for time-to-event regression, and R^2 coefficient for regression. For comparison, we present the relative performance gain over the NTP baseline for the best method in each loss family. When evaluating the pretrained models, we generate feature embeddings for each task cohort and fit a task-specific head (logistic regression for binary classification, Deephit for time-to-event tasks,

and linear regression for regression tasks). Detailed model performance is provided in Appendix B.

6. Results

Figures 2 and 3 present the relative gain for both architectures across all tasks trained and evaluated on the MIMIC-IV and CUMC. For each loss, we compare relative gain with respect to the best ‘in-class’ model. That is, the relative gain of TPP will report the best performance among Transformer with TPP loss, Mamba with TPP loss, and MOTOR, relative to the best NTP model to underscore the impact of the proposed loss relative to NTP.

ORA improves binary classification. We evaluate binary classification tasks using the Transformer backbone across MIMIC-IV and CUMC. In Figure 2, NTP loss outperforms the traditional machine learning paradigm in the majority of binary tasks, as shown by the comparison between the task-specific baseline and NTP. Critically, ORA consistently improves over NTP on every classification task in both datasets: most tasks gain between 2 and 5% in AUROC, and a large improvement on Celiac (+20%) on the CUMC dataset. ORA also consistently outperforms the TPP objec-

tive, indicating that explicitly modeling event marks yields benefits beyond predicting numerical value.

ORA improves time-to-event prediction and linear-probe regression. Beyond the traditional evaluation benchmark, our work introduces time-to-event and regression tasks to assess FMs’ capacity to capture patients’ health beyond binary outcomes. When focusing on time-to-event tasks, both TPP and ORA lead to improved performance compared to NTP with an average gain of 5.9% for Transformers. Even though TPP is explicitly designed for time-to-event prediction, ORA still outperforms it in most time-to-event tasks (5 out of 7), demonstrating that modeling the joint with the observed values is predictive of some phenotypes. For regression tasks, the proposed method is the only loss that consistently outperforms NTP across all tasks, yielding an average 33.6%[+2.5–93.9%] improvement. Note that the last imputation for laboratory results outperforms FMs in Creatinine and Platelets, but underperforms in Oxygen, likely due to the high fluctuation of oxygen measurement. Meanwhile, ORA reduces the gap relative to this baseline, confirming that a loss function that accounts for observed values is critical for improving performance in this setting.

ORA generalizes across architectures, tasks, and datasets. An essential dimension of our experimentation is the consideration of 2 architectures, 14 tasks, and 2 datasets, allowing external validation of our findings. While the previous conclusions focus on Transformers, similar conclusions can be made for Mamba architectures, as shown in Figure 3. For classification tasks, training Mamba with ORA consistently outperforms NTP on most tasks by 2 – 17%, with slightly worse performance –8.2% on Stroke. Since prior occurrences are highly predictive, it is likely that using NTP loss or even an XGBoost model is capable of predicting a future occurrence. For time-to-event prediction, the proposed loss improves over NTP in all tasks except Stroke by 0.9 – 9.6%. In regression, ORA shows a large improvement over NTP, achieving on average a performance gain of 38.3%[+5.3–110.9%]. Compared with TPP or the last imputation baseline, the proposed loss yields the highest R^2 on half of the tasks across both datasets (3 out of 6). These results reinforce that ORA generalizes well for all tasks for both Transformer and Mamba architectures.

7. Discussion

Our work introduces ORA, a novel pretraining loss that accounts for temporal irregularity and numerical values associated with EHR events. While previous works have proposed approaches to account for these dimensions through tokenization and the choice of pretraining losses (Burger et al., 2025; Gadd et al., 2025), no work isolates the sources of relative improvements across diverse and clinically-meaningful

downstream tasks. Our core contribution is to demonstrate that the choice of pretraining loss alone is responsible for a critical improvement in the generalizability of FMs. The current literature on FMs often focuses on novel architectures, with design choices driven by performance. Isolating the impact of these choices has seldom been studied, yet it is critical for further advancement in EHR FMs. Our contribution aims to advance the mathematical foundation of these models and, consequently, inform the development of future ones. Furthermore, we extend linear-probe evaluation beyond classification to include time-to-event modeling and regression. ORA, which captures EHR temporal irregularities and their associated values in the pretraining loss, improves performance across the broadest range of downstream tasks, regardless of model architecture, across multiple datasets.

While ORA consistently improves performance across a broad range of tasks, when combined with specific tokenization strategies and depending on task difficulty, model performance is not universally optimal. Based on the empirical results, ORA may be an overkill for conditions with frequent prior occurrences, when simpler objectives such as NTP already capture much of the predictive signal. ORA is primarily relevant when the underlying data-generating process is a marked point process, such as EHR data.

Limitations and future work. Our evaluation focuses on generalizability. Given prior evidence that multi-task training improves robustness under distribution shift (Jeanselme et al., 2025; Burger et al., 2025), an important direction for future work is to assess ORA’s pretraining using multiple datasets, to enable the promises of FMs in healthcare.

Another limitation concerns the choice of discretization. Although quantile-based discretization accommodates substantial distributional variability, it may inadequately capture sharply peaked distributions, as observed in regression where FMs do not always capture Creatinine variability. Combining ORA with more expressive and adaptive discretization may improve flexibility efficiently.

Meanwhile, we fix the model capacity at approximately 120M parameters and evaluate all models on two datasets with different scales. While we demonstrate that ORA outperforms NTP in most tasks, it remains an open question how these gains scale with model size. Future work should examine whether the observed improvements persist or change as we increase the model parameters.

Finally, our study focuses on linear probing. Extending the evaluation to fine-tuning may clarify how downstream adaptation interacts with the proposed loss. Nevertheless, modeling the joint distribution is particularly advantageous in low-supervision regimes and yields strong performance under linear probing, which is crucial as models become

larger and even fine-tuning becomes computationally intensive.

Impact Statement

Foundation models in healthcare promise to democratize access to advanced modeling capabilities for institutions lacking the resources to build models from scratch. Yet this promise comes with risks to privacy, fairness, and safety. Although this paper advances the mathematical foundations of these models, such risks must be rigorously addressed before any clinical implementation.

Acknowledgments

VJ, and SJ would like to acknowledge partial support from NIH 5R01MH137679-02. AK would like to acknowledge the support of NIH 5T15LM007079-34. ZJ and SJ would like to acknowledge partial support from NIH 5R01LM014380-02. SJ and ZJ would like to acknowledge partial support from the Google Research Scholar Award. SAL would like to acknowledge the generous support of the Warren Alpert Foundation, Warren Alpert-UCLA Computational Biology/AI (CBAI) Scholar Training and Retention Program (award 20242540). SJ would like to acknowledge partial support from the SNF Center for Precision Psychiatry & Mental Health, Columbia. Any opinions, findings, conclusions, or recommendations in this manuscript are those of the authors and do not reflect the views, policies, endorsements, expressed or implied, of any aforementioned funding agencies/institutions.

References

Alaa, A. M., Hu, S., and Schaar, M. Learning from clinical judgments: Semi-markov-modulated marked hawkes processes for risk prognosis. In *International conference on machine learning*, pp. 60–69. PMLR, 2017.

An, U., Lee, S. A., Jeong, M., Gorla, A., Chiang, J. N., and Sankararaman, S. Dk-behrt: Teaching language models international classification of disease (icd) codes using known disease descriptions. In *AAAI Bridge Program on AI for Medicine and Healthcare*, pp. 133–143. PMLR, 2025.

Ansari, A. F., Stella, L., Turkmen, C., Zhang, X., Mercado, P., Shen, H., Shchur, O., Rangapuram, S. S., Arango, S. P., Kapoor, S., et al. Chronos: Learning the language of time series. *arXiv preprint arXiv:2403.07815*, 2024.

Antolini, L., Boracchi, P., and Biganzoli, E. A time-dependent discrimination index for survival data. *Statistics in medicine*, 24(24), 2005.

Bhave, S. and Perotte, A. Point processes for competing observations with recurrent networks (popcorn): A generative model of ehr data. In *Machine Learning for Healthcare Conference*, pp. 770–789. PMLR, 2021.

Burger, M., Chopard, D., Londschen, M., Sergeev, F., Yéche, H., Kuznetsova, R., Faltys, M., Gerdes, E., Leshetkina, P., Bühlmann, P., et al. A foundation model for intensive care: Unlocking generalization across tasks and domains at scale. *medRxiv*, pp. 2025–07, 2025.

Burkhart, M. C., Ramadan, B., Liao, Z., Chhikara, K., Rojas, J. C., Parker, W. F., and Beaulieu-Jones, B. K. Foundation models for electronic health records: representation dynamics and transferability. *arXiv preprint arXiv:2504.10422*, 2025.

Chang, C., Wang, W.-Y., Peng, W.-C., and Chen, T.-F. Llm4ts: Aligning pre-trained llms as data-efficient time-series forecasters. *ACM Transactions on Intelligent Systems and Technology*, 16(3):1–20, 2025a.

Chang, Y., Boyd, A. J., Xiao, C., Kass-Hout, T., Bhatia, P., Smyth, P., and Warrington, A. Deep continuous-time state-space models for marked event sequences. In *The Thirty-ninth Annual Conference on Neural Information Processing Systems*, 2025b.

Chen, G. H. et al. An introduction to deep survival analysis models for predicting time-to-event outcomes. *Foundations and Trends® in Machine Learning*, 17(6):921–1100, 2024.

Chen, T. and Guestrin, C. Xgboost: A scalable tree boosting system. In *Proceedings of the 22nd ACM SIGKDD International Conference on Knowledge Discovery and Data Mining*, KDD ’16, pp. 785–794. ACM, August 2016.

Cui, H., Unell, A., Chen, B., Fries, J. A., Alsentzer, E., Koyejo, S., and Shah, N. H. Timer: Temporal instruction modeling and evaluation for longitudinal clinical records. *NPJ Digital Medicine*, 8(1):577, 2025.

Daley, D. J. and Vere-Jones, D. *An introduction to the theory of point processes: volume I: elementary theory and methods*. Springer, 2003.

Das, A., Kong, W., Sen, R., and Zhou, Y. A decoder-only foundation model for time-series forecasting. In *Forty-first International Conference on Machine Learning*, 2024.

Devlin, J., Chang, M.-W., Lee, K., and Toutanova, K. Bert: Pre-training of deep bidirectional transformers for language understanding. In *Proceedings of the 2019 conference of the North American chapter of the association for computational linguistics: human language technologies, volume 1 (long and short papers)*, pp. 4171–4186, 2019.

Du, N., Dai, H., Trivedi, R., Upadhyay, U., Gomez-Rodriguez, M., and Song, L. Recurrent marked temporal point processes: Embedding event history to vector. In *Proceedings of the 22nd ACM SIGKDD international conference on knowledge discovery and data mining*, pp. 1555–1564, 2016.

Enguehard, J., Busbridge, D., Bozson, A., Woodcock, C., and Hammerla, N. Neural temporal point processes for modelling electronic health records. In *Machine Learning for Health*, pp. 85–113. PMLR, 2020.

Fallahpour, A., Alinoori, M., Ye, W., Cao, X., Afkampour, A., and Krishnan, A. Ehrmamba: Towards generalizable and scalable foundation models for electronic health records. *arXiv preprint arXiv:2405.14567*, 2024.

Gadd, C., Gokhale, K., Acharya, A., Cooper, J., Crowe, F., Fitzsimmons, L., Jackson, T., Nirantharakumar, K., Yau, C., and collaborative, O. Survivehr: a competing risks, time-to-event foundation model for multiple long-term conditions from primary care electronic health records. *medRxiv*, pp. 2025–08, 2025.

Goswami, M., Szafer, K., Choudhry, A., Cai, Y., Li, S., and Dubrawski, A. Moment: A family of open time-series foundation models. *arXiv preprint arXiv:2402.03885*, 2024.

Gu, A. and Dao, T. Mamba: Linear-time sequence modeling with selective state spaces. *arXiv preprint arXiv:2312.00752*, 2023.

Gu, A. and Dao, T. Mamba: Linear-time sequence modeling with selective state spaces. In *First conference on language modeling*, 2024.

Guo, L. L., Steinberg, E., Fleming, S. L., Posada, J., Lemmon, J., Pfohl, S. R., Shah, N., Fries, J., and Sung, L. Ehr foundation models improve robustness in the presence of temporal distribution shift. *Scientific Reports*, 13(1): 3767, 2023.

Guo, L. L., Fries, J., Steinberg, E., Fleming, S. L., Morse, K., Aftandilian, C., Posada, J., Shah, N., and Sung, L. A multi-center study on the adaptability of a shared foundation model for electronic health records. *NPJ digital medicine*, 7(1):171, 2024.

Hegselmann, S., Buendia, A., Lang, H., Agrawal, M., Jiang, X., and Sontag, D. Tabllm: Few-shot classification of tabular data with large language models. In *International Conference on Artificial Intelligence and Statistics*, pp. 5549–5581. PMLR, 2023.

Hegselmann, S., von Arnim, G., Rheude, T., Kronenberg, N., Sontag, D., Hindricks, G., Eils, R., and Wild, B. Large language models are powerful electronic health record encoders. *arXiv preprint arXiv:2502.17403*, 2025.

Hill, B. L., Emami, M., Nori, V. S., Cordova-Palomera, A., Tillman, R. E., and Halperin, E. Chiron: a generative foundation model for structured sequential medical data. 2023.

Hripcsak, G., Shang, N., Peissig, P. L., Rasmussen, L. V., Liu, C., Benoit, B., Carroll, R. J., Carrell, D. S., Denny, J. C., Dikilitas, O., et al. Facilitating phenotype transfer using a common data model. *Journal of biomedical informatics*, 96:103253, 2019.

Hur, K., Oh, J., Kim, J., Kim, J., Lee, M. J., Cho, E., Moon, S.-E., Kim, Y.-H., Atallah, L., and Choi, E. Genhpf: General healthcare predictive framework for multi-task multi-source learning. *IEEE Journal of Biomedical and Health Informatics*, 28(1):502–513, 2023.

Islam, K. T., Shelton, C. R., Casse, J. I., and Wetzel, R. Marked point process for severity of illness assessment. In *Machine learning for healthcare conference*, pp. 255–270. PMLR, 2017.

Jeanselme, V. *Clinical Presence: Impact on Predictive Modelling and Algorithmic Fairness*. PhD thesis, University of Cambridge (United Kingdom), 2024.

Jeanselme, V., Yoon, C. H., Tom, B., and Barrett, J. Neural fine-gray: Monotonic neural networks for competing risks. In *Conference on Health, Inference, and Learning*, pp. 379–392. PMLR, 2023.

Jeanselme, V., Martin, G., Sperrin, M., Peek, N., Tom, B., and Barrett, J. Prediction of survival outcomes under clinical presence shift: A joint neural network architecture. *arXiv preprint arXiv:2508.05472*, 2025.

Jin, M., Wang, S., Ma, L., Chu, Z., Zhang, J. Y., Shi, X., Chen, P.-Y., Liang, Y., Li, Y.-F., Pan, S., et al. Time-llm: Time series forecasting by reprogramming large language models. *arXiv preprint arXiv:2310.01728*, 2023.

Johnson, A. E., Bulgarelli, L., Shen, L., Gayles, A., Shamamoto, A., Horng, S., Pollard, T. J., Hao, S., Moody, B., Gow, B., et al. Mimic-iv, a freely accessible electronic health record dataset. *Scientific data*, 10(1):1, 2023.

Karami, H., Atienza, D., and Ionescu, A. Tee4ehr: Transformer event encoder for better representation learning in electronic health records. *Artificial Intelligence in Medicine*, 154:102903, 2024.

Lee, C., Zame, W., Yoon, J., and Van Der Schaar, M. Deephit: A deep learning approach to survival analysis with competing risks. In *Proceedings of the AAAI conference on artificial intelligence*, volume 32, 2018.

Lee, S. A., Jain, S., Chen, A., Ono, K., Fang, J., Rudas, A., and Chiang, J. N. Emergency department decision support using clinical pseudo-notes. *arXiv preprint arXiv:2402.00160*, 2024.

Lee, S. A., Jain, S., Chen, A., Ono, K., Biswas, A., Rudas, Á., Fang, J., and Chiang, J. N. Clinical decision support using pseudo-notes from multiple streams of ehr data. *npj Digital Medicine*, 8(1):394, 2025.

Li, Y., Rao, S., Solares, J. R. A., Hassaine, A., Ramakrishnan, R., Canoy, D., Zhu, Y., Rahimi, K., and Salimi-Khorshidi, G. Behrt: transformer for electronic health records. *Scientific reports*, 10(1):7155, 2020.

McDermott, M., Nestor, B., Argaw, P., and Kohane, I. S. Event stream gpt: a data pre-processing and modeling library for generative, pre-trained transformers over continuous-time sequences of complex events. *Advances in Neural Information Processing Systems*, 36:24322–24334, 2023.

Mei, H. and Eisner, J. M. The neural hawkes process: A neurally self-modulating multivariate point process. *Advances in neural information processing systems*, 30, 2017.

Odgaard, M., Klein, K. V., Thysen, S. M., Jimenez-Solem, E., Sillesen, M., and Nielsen, M. Core-behrt: A carefully optimized and rigorously evaluated behrt. *arXiv preprint arXiv:2404.15201*, 2024.

Omi, T., Aihara, K., et al. Fully neural network based model for general temporal point processes. *Advances in neural information processing systems*, 32, 2019.

Pang, C., Jiang, X., Kalluri, K. S., Spotnitz, M., Chen, R., Perotte, A., and Natarajan, K. Cehr-bert: Incorporating temporal information from structured ehr data to improve prediction tasks. In Roy, S., Pfohl, S., Rocheteau, E., Tadesse, G. A., Oala, L., Falck, F., Zhou, Y., Shen, L., Zamzmi, G., Mugambi, P., Zirikly, A., McDermott, M. B. A., and Alsentzer, E. (eds.), *Proceedings of Machine Learning for Health*, volume 158 of *Proceedings of Machine Learning Research*, pp. 239–260. PMLR, 04 Dec 2021. URL <https://proceedings.mlr.press/v158/pang21a.html>.

Pang, C., Jiang, X., Pavinkurve, N. P., Kalluri, K. S., Minto, E. L., Patterson, J., Zhang, L., Hripcak, G., Gürsoy, G., Elhadad, N., et al. Cehr-gpt: Generating electronic health records with chronological patient timelines. *arXiv preprint arXiv:2402.04400*, 2024.

Pang, C., Jeanselme, V., Choi, Y. S., Jiang, X., Jing, Z., Kashyap, A., Kobayashi, Y., Li, Y., Pollet, F., Natarajan, K., et al. Fomoh: A clinically meaningful foundation model evaluation for structured electronic health records. *arXiv preprint arXiv:2505.16941*, 2025.

Rasmy, L., Xiang, Y., Xie, Z., Tao, C., and Zhi, D. Medbert: pretrained contextualized embeddings on large-scale structured electronic health records for disease prediction. *NPJ digital medicine*, 4(1):86, 2021.

Ren, W., Zhu, J., Liu, Z., Zhao, T., and Honavar, V. A comprehensive survey of electronic health record modeling: From deep learning approaches to large language models. *arXiv preprint arXiv:2507.12774*, 2025.

Schulam, P. and Saria, S. Reliable decision support using counterfactual models. *Advances in neural information processing systems*, 30, 2017.

Shmatko, A., Jung, A. W., Gaurav, K., Brunak, S., Mortensen, L. H., Birney, E., Fitzgerald, T., and Gerstung, M. Learning the natural history of human disease with generative transformers. *Nature*, 647(8088):248–256, 2025.

Snyder, D. L. and Miller, M. I. *Random point processes in time and space*. Springer Science & Business Media, 2012.

Steinberg, E., Jung, K., Fries, J. A., Corbin, C. K., Pfohl, S. R., and Shah, N. H. Language models are an effective representation learning technique for electronic health record data. *Journal of biomedical informatics*, 113: 103637, 2021.

Steinberg, E., Xu, Y., Fries, J. A., and Shah, N. MOTOR: A time-to-event foundation model for structured medical records. In *The Twelfth International Conference on Learning Representations*, 2024. URL <https://openreview.net/forum?id=Nialiwi2V6>.

Su, X., Messica, S., Huang, Y., Johnson, R., Fesser, L., Gao, S., Sahneh, F., and Zitnik, M. Multimodal medical code tokenizer. *arXiv preprint arXiv:2502.04397*, 2025.

Vaswani, A., Shazeer, N., Parmar, N., Uszkoreit, J., Jones, L., Gomez, A. N., Kaiser, Ł., and Polosukhin, I. Attention is all you need. *Advances in neural information processing systems*, 30, 2017.

Vincent, J.-L., Moreno, R., Takala, J., Willatts, S., De Mendonça, A., Bruining, H., Reinhart, C. K., Suter, P., and Thijs, L. G. The sofa (sepsis-related organ failure assessment) score to describe organ dysfunction/failure: On behalf of the working group on sepsis-related problems of the european society of intensive care medicine (see contributors to the project in the appendix). *Intensive care medicine*, 22(7):707–710, 1996.

Wornow, M., Xu, Y., Thapa, R., Patel, B., Steinberg, E., Fleming, S., Pfeffer, M. A., Fries, J., and Shah, N. H. The shaky foundations of large language models and foundation models for electronic health records. *npj digital medicine*, 6(1):135, 2023.

Wornow, M., Bedi, S., Hernandez, M. A. F., Steinberg, E., Fries, J. A., Ré, C., Koyejo, S., and Shah, N. H. Context clues: Evaluating long context models for clinical prediction tasks on ehrs. *arXiv preprint arXiv:2412.16178*, 2024a.

Wornow, M., Thapa, R., Steinberg, E., Fries, J., and Shah, N. Ehrshot: An ehr benchmark for few-shot evaluation of foundation models. *Advances in Neural Information Processing Systems*, 36, 2024b.

A. Experimental setting

A.1. Datasets

Table 1. Dataset Split of MIMIC-IV and CUMC

Split Name	MIMIC-IV		CUMC	
	# Patients	# Events	# Patients	# Events
Training Set	291,702	579,667,440	3,996,578	1,562,316,866
Tuning Set	36463	71,789,378	705,279	273,247,565
Test Set	36462	71,290,747	2,015,082	781,462,164

A.2. Cohort Definition

A.2.1. OUTCOME DEFINITION

We construct three outcome tasks using the same definitions as in (Pang et al., 2025). The detailed inclusion criteria can be found in section 3.2 of the referenced paper.

A.2.2. PHENOTYPE DEFINITION

For each disease, we define a set of at-risk events as cohort inclusion criteria and a set of case events to determine patients' labels. Compared with using a set of ICD codes, this method adds more task difficulty and is more clinically meaningful.

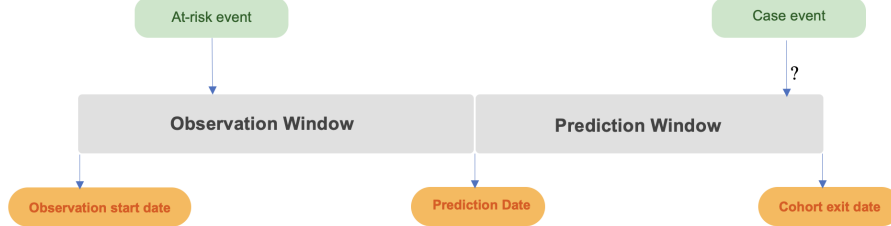


Figure 4. Visualization of Cohort Definition. The detailed definition of at-risk, prediction time, and case events can be found in Appendix B of (Pang et al., 2025).

A.2.3. REGRESSION DEFINITION

We define regression tasks as predicting the lab test after 4 hours of the prediction time. Each lab event can be identified with a corresponding code in the following table:

Table 2. Corresponding Medical Codes for All Regression Tasks on MIMIC and CUMC

Task	MIMIC-IV	CUMC(OMOP)
Creatinine	50912	LOINC/2160-0
Platelets	51265	LOINC/26515-7
Oxygen	50821 (PaO_2)	LOINC/2708-6 (SpO_2)

A.3. Model

A.3.1. TOKENIZER

We use an entropy-based filter similar to (Steinberg et al., 2024). Instead of taking the most frequent events in the vocabulary, we select codes with the highest entropy over the whole dataset. Define $p(m)$ as the probability that the code appears in each patient. The entropy calculation is as follows:

$$H(m) = -p(m)\log(m)$$

If the dataset has an ontology mapping, we can calculate the conditional entropy of any code m relative to its parent n . Suppose $p(m, n^+)$ denotes the probability that both m and n appear per patient and $p(m, n^-)$ be the probability that only m appears in the patient. $p(m) = p(m, n^+) + p(m, n^-)$, the conditional entropy is as follows:

$$H(m|n) = -p(m, n^-)\log\frac{p(m, n^-)}{p(m)} - p(m, n^+)\log\frac{p(m, n^+)}{p(m)}$$

A.3.2. MODEL CONFIGURATIONS

For a fair comparison across different architectures, we set the parameter size for all models to around 120M. Within each architecture, we also use the same configuration files for different losses, which is specified as follows:

Table 3. Model configurations.

Model	Configuration	Value
Transformer	context length	8192
	learning rate	1e-5
	dim model	768
	intermediate size	3072
	num layers	11
	num heads	12
	Total Parameters	119M
Mamba	context length	8192
	learning rate	2e-4
	dim model	768
	intermediate size	1536
	num layers	28
	num layers	16
	Total Parameters	120M

A.3.3. EFFICIENT PREDICTION HEAD

The last layer of Transformer and Mamba produces an embedding matrix $X \in R^{D \times D}$. We need to project it into the final probability matrix $P(x)$ for both nonnumerical codes (eg, diagnosis) and numerical codes with continuous values (eg, lab test). As mentioned in the main paper, we adopt a two-stage projection to be parameter efficient. D indicates the embedding dimension after Transformer or Mamba. D_2 is the hidden dimension after the first projection layer. M_{non} and M_{num} represent nonnumerical codes and numerical codes for pretraining, respectively. The visualization is as follows:

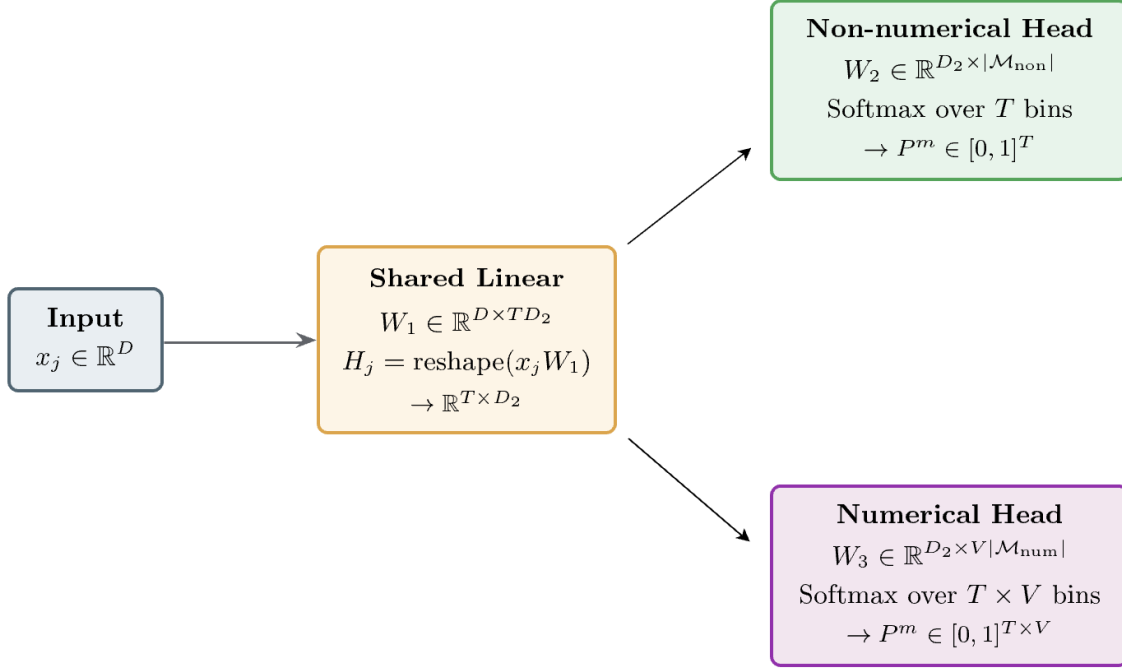


Figure 5. Efficient prediction head: We share the same projection layer for both nonnumerical and numerical codes and then use two different projection heads to output the separate probability matrices.

B. Experiment Results

This section details the performance for each architecture, loss, and task across both datasets.

B.1. MIMIC-IV

We evaluate all models on 6 classification tasks, 3 time-to-event tasks and 3 regression tasks on MIMIC-IV.

B.1.1. CLASSIFICATION

Table 4. AUROC of Binary Classification Tasks for MIMIC-IV Patients. *Larger is better.*

Model	Readmission	LOS	Mortality	AMI	MASLD	Stroke
XGBoost	0.726 (0.003)	0.748 (0.003)	0.882 (0.005)	0.807 (0.008)	0.700 (0.020)	0.708 (0.023)
CC-Llama	0.730 (0.003)	0.781 (0.003)	0.901 (0.005)	0.796 (0.010)	0.663 (0.020)	0.696 (0.025)
CC-Mamba	0.731 (0.003)	0.779 (0.003)	0.896 (0.006)	0.783 (0.009)	0.661 (0.019)	0.665 (0.024)
MOTOR	0.743 (0.002)	0.833 (0.002)	0.954 (0.0023)	0.825 (0.008)	0.703 (0.021)	0.710 (0.019)
Transformer-NTP	0.728 (0.003)	0.808 (0.002)	0.926 (0.004)	0.810 (0.008)	0.691 (0.020)	0.691 (0.025)
Transformer-TPP	0.744 (0.004)	0.839 (0.002)	0.963 (0.003)	0.818 (0.007)	0.705 (0.018)	0.700 (0.020)
Transformer-ORA	0.745 (0.003)	0.841 (0.002)	0.965 (0.002)	0.827 (0.007)	0.714 (0.017)	0.711 (0.018)
Mamba-NTP	0.732 (0.004)	0.813 (0.002)	0.933 (0.004)	0.814 (0.008)	0.679 (0.020)	0.719 (0.022)
Mamba-TPP	0.741 (0.003)	0.809 (0.003)	0.934 (0.004)	0.822 (0.007)	0.709 (0.020)	0.666 (0.017)
Mamba-ORA	0.747 (0.003)	0.812 (0.002)	0.939 (0.004)	0.832 (0.007)	0.722 (0.020)	0.660 (0.022)

B.1.2. TIME-TO-EVENT

 Table 5. C-index of Time-to-event Phenotype Tasks for MIMIC-IV Patients. *Larger is better.*

Model	AMI	MASLD	Stroke
Deephit	0.651 (0.029)	0.560 (0.024)	0.574 (0.085)
CC-Llama	0.782 (0.030)	0.687 (0.023)	0.847 (0.039)
CC-Mamba	0.760 (0.035)	0.664 (0.021)	0.845 (0.039)
MOTOR	0.798 (0.027)	0.696 (0.018)	0.828 (0.035)
<hr/>			
Transformer-NTP	0.760 (0.034)	0.679 (0.018)	0.767 (0.064)
Transformer-TPP	0.839 (0.028)	0.702 (0.019)	0.899 (0.023)
Transformer-ORA	0.819 (0.029)	0.735 (0.016)	0.899 (0.024)
<hr/>			
Mamba-NTP	0.773 (0.030)	0.667 (0.018)	0.743 (0.064)
Mamba-TPP	0.844 (0.029)	0.739 (0.017)	0.825 (0.034)
Mamba-ORA	0.847 (0.029)	0.703 (0.019)	0.837 (0.034)

B.1.3. REGRESSION

 Table 6. R^2 of Lab Test Regression for MIMIC-IV Patients. *Larger coefficient reflects a larger proportion of variance explained.*

Model	Creatinine	PaO2	Platelets
CC-Llama	0.319 (0.018)	0.219 (0.005)	0.290 (0.004)
	0.307 (0.017)	0.218 (0.005)	0.261 (0.004)
CC-Mamba	0.556 (0.033)	0.231 (0.005)	0.298 (0.004)
	0.877 (0.034)	-0.431 (0.024)	0.910 (0.002)
Most Recent			
Transformer-NTP	0.489 (0.025)	0.259 (0.005)	0.312 (0.004)
	0.603 (0.030)	0.234 (0.005)	0.310 (0.003)
Transformer-TPP	0.603 (0.028)	0.267 (0.005)	0.605 (0.003)
Mamba-NTP	0.595 (0.029)	0.270 (0.005)	0.407 (0.003)
	0.617 (0.030)	0.241 (0.005)	0.400 (0.004)
Mamba-TPP	0.645 (0.034)	0.286 (0.006)	0.659 (0.003)
Mamba-ORA			

 Table 7. RMSE of Lab Test Regression for MIMIC-IV Patients. *Lower is better.*

Model	Creatinine	PaO2	Platelets
Baseline	0.503 (0.084)	77.727 (0.535)	38.632 (0.326)
	1.244 (0.053)	57.369 (0.466)	108.897 (0.653)
CC-Llama	1.255 (0.052)	57.421 (0.462)	111.113 (0.635)
	0.968 (0.067)	56.920 (0.447)	108.285 (0.630)
MOTOR			
Transformer-NTP	1.038 (0.058)	55.888 (0.461)	107.198 (0.647)
	0.915 (0.063)	56.816 (0.452)	107.359 (0.605)
Transformer-TPP	0.915 (0.062)	55.576 (0.439)	81.202 (0.593)
Mamba-NTP	0.925 (0.062)	55.475 (0.451)	99.533 (0.632)
	0.899 (0.064)	56.549 (0.447)	100.106 (0.567)
Mamba-TPP	0.866 (0.068)	54.877 (0.429)	75.476 (0.581)
Mamba-ORA			

Table 8. MAE of Lab Test Regression for MIMIC-IV Patients. *Lower is better.*

Model	Creatinine	PaO2	Platelets
Baseline	0.193 (0.002)	45.537 (0.324)	25.184 (0.136)
CC-Llama	0.803 (0.004)	38.620 (0.230)	78.139 (0.312)
CC-Mamba	0.811 (0.004)	38.593 (0.219)	80.145 (0.317)
MOTOR	0.542 (0.004)	38.211 (0.206)	77.215 (0.322)
Transformer-NTP	0.651 (0.004)	37.102 (0.218)	76.247 (0.310)
Transformer-TPP	0.507 (0.003)	38.114 (0.217)	76.565 (0.310)
Transformer-ORA	0.504 (0.003)	36.859 (0.209)	56.163 (0.249)
Mamba-NTP	0.547 (0.003)	36.983 (0.209)	70.657 (0.284)
Mamba-TPP	0.492 (0.003)	37.667 (0.207)	70.825 (0.277)
Mamba-ORA	0.448 (0.003)	36.319 (0.199)	51.451 (0.236)

B.2. CUMC

As external validation, this section shows similar results across tasks and architectures on the CUMC dataset, a large urban center.

B.2.1. CLASSIFICATION

Table 9. AUROC of Binary Classification Tasks for CUMC Patients. *Larger is better.*

Model	Readmission	LOS	Mortality	AMI	MASLD	Stroke	Celiac
XGBoost	0.732	0.773	0.875	0.833	0.681	0.872	0.650
	(0.003)	(0.002)	(0.005)	(0.008)	(0.009)	(0.006)	(0.031)
Llama	0.758	0.798	0.892	0.821	0.731	0.846	0.604
	(0.003)	(0.002)	(0.004)	(0.009)	(0.008)	(0.007)	(0.040)
Mamba	0.757	0.784	0.883	0.816	0.706	0.865	0.635
	(0.003)	(0.002)	(0.004)	(0.009)	(0.008)	(0.007)	(0.038)
MOTOR	0.783	0.850	0.963	0.853	0.727	0.869	0.647
	(0.003)	(0.002)	(0.002)	(0.007)	(0.007)	(0.006)	(0.030)
Transformer-NTP	0.760	0.842	0.938	0.821	0.713	0.849	0.624
	(0.003)	(0.002)	(0.003)	(0.008)	(0.009)	(0.007)	(0.039)
Transformer-TPP	0.784	0.857	0.963	0.843	0.718	0.863	0.736
	(0.003)	(0.002)	(0.002)	(0.008)	(0.008)	(0.006)	(0.033)
Transformer-ORA	0.787	0.866	0.968	0.850	0.745	0.870	0.749
	(0.003)	(0.002)	(0.002)	(0.008)	(0.007)	(0.007)	(0.036)
Mamba-NTP	0.757	0.817	0.915	0.780	0.681	0.830	0.637
	(0.003)	(0.002)	(0.003)	(0.010)	(0.008)	(0.007)	(0.033)
Mamba-TPP	0.776	0.859	0.942	0.854	0.737	0.864	0.739
	(0.003)	(0.002)	(0.003)	(0.008)	(0.008)	(0.006)	(0.034)
Mamba-ORA	0.779	0.861	0.946	0.858	0.766	0.873	0.744
	(0.002)	(0.002)	(0.003)	(0.008)	(0.008)	(0.006)	(0.038)

B.2.2. TIME-TO-EVENT

 Table 10. C-index of Time-to-event Phenotype Tasks for CUMC Patients. *Larger is better.*

Model	AMI	Celiac	Ischemic Stroke	MASLD
Deephit	0.617 (0.009)	0.564 (0.029)	0.626 (0.009)	0.601 (0.005)
	0.719 (0.007)	0.581 (0.022)	0.780 (0.006)	0.620 (0.006)
CC-Llama	0.732 (0.008)	0.673 (0.018)	0.773 (0.006)	0.603 (0.006)
	0.752 (0.007)	0.593 (0.023)	0.760 (0.007)	0.624 (0.005)
MOTOR	0.683 (0.007)	0.582 (0.026)	0.727 (0.008)	0.605 (0.006)
	0.729 (0.008)	0.577 (0.023)	0.748 (0.007)	0.616 (0.005)
Transformer-ORA	0.721 (0.009)	0.604 (0.020)	0.769 (0.006)	0.626 (0.005)
	0.693 (0.008)	0.519 (0.024)	0.721 (0.008)	0.613 (0.005)
Mamba-TPP	0.739 (0.008)	0.641 (0.023)	0.758 (0.008)	0.603 (0.005)
	0.747 (0.007)	0.679 (0.021)	0.767 (0.007)	0.637 (0.006)

B.2.3. REGRESSION

 Table 11. R^2 of Lab Test Regression for CUMC Patients. *Larger coefficient reflects a larger proportion of variance explained.*

Model	Creatinine	Platelets	SpO2
Most Recent	0.679	0.426	0.078
	(0.036)	(0.011)	(0.013)
CC-Llama	0.298	0.150	0.770
	(0.013)	(0.005)	(0.007)
CC-Mamba	0.277	0.146	0.762
	(0.013)	(0.006)	(0.007)
MOTOR	0.469	0.198	0.842
	(0.020)	(0.007)	(0.006)
Transformer-NTP	0.431	0.228	0.816
	(0.022)	(0.006)	(0.007)
Transformer-TPP	0.397	0.203	0.832
	(0.018)	(0.007)	(0.006)
Transformer-ORA	0.542	0.349	0.836
	(0.024)	(0.008)	(0.006)
Mamba-NTP	0.423	0.220	0.809
	(0.024)	(0.007)	(0.006)
Mamba-TPP	0.543	0.311	0.849
	(0.027)	(0.008)	(0.006)
Mamba-ORA	0.582	0.464	0.852
	(0.029)	(0.007)	(0.006)

 Table 12. RMSE of Lab Test Regression for CUMC Patients. *Lower is better.*

Model	Creatinine	Platelets	SpO2
Most Recent	0.630	74.419	15.598
	(0.047)	(1.048)	(0.225)
CC-Llama	0.987	90.486	7.802
	(0.035)	(0.941)	(0.114)
CC-Mamba	1.001	90.695	7.939
	(0.035)	(0.939)	(0.112)
MOTOR	0.825	88.308	6.437
	(0.042)	(0.948)	(0.123)
Transformer-NTP	0.856	86.837	6.948
	(0.039)	(0.969)	(0.110)
Transformer-TPP	0.879	88.046	6.638
	(0.041)	(0.936)	(0.117)
Transformer-ORA	0.766	79.574	6.555
	(0.044)	(0.883)	(0.122)
Mamba-NTP	0.860	87.097	7.078
	(0.045)	(0.881)	(0.110)
Mamba-TPP	0.765	81.869	6.301
	(0.047)	(0.911)	(0.123)
Mamba-ORA	0.732	72.188	6.226
	(0.047)	(0.878)	(0.118)

Table 13. MAE of Lab Test Regression for CUMC Patients. *Lower is better.*

Model	Creatinine	Platelets	SpO2
Most Recent	0.235 (0.004)	47.591 (0.428)	6.377 (0.112)
CC-Llama	0.567 (0.006)	65.073 (0.458)	4.670 (0.046)
CC-Mamba	0.567 (0.006)	65.327 (0.488)	4.742 (0.045)
MOTOR	0.402 (0.006)	63.290 (0.478)	3.325 (0.038)
Transformer-NTP	0.445 (0.005)	62.540 (0.436)	3.968 (0.037)
Transformer-TPP	0.406 (0.006)	63.068 (0.435)	3.448 (0.037)
Transformer-ORA	0.341 (0.005)	56.882 (0.376)	3.377 (0.040)
Mamba-NTP	0.434 (0.006)	62.555 (0.393)	4.086 (0.039)
Mamba-TPP	0.340 (0.005)	58.465 (0.407)	3.196 (0.038)
Mamba-ORA	0.326 (0.005)	49.793 (0.357)	3.103 (0.037)